Short Subsurface Cracks Under Conditions of Slip and Stick Caused by a Moving Compressive Load

S. Sheppard
Student Mem. ASME

J. R. Barber

M. Comninou
Mem. ASME

Department of Mechanical Engineering
and Applied Mechanics,
University of Michigan,
Ann Arbor, Mich. 48109

The mechanism of spalling failure in rolling contact is modeled by an elastic half-plane with a subsurface crack parallel to the surface, loaded by a compressive normal force which moves over the surface. Coulomb friction at the crack faces reduces the Mode II Stress Intensity Factors and results in a number of history-dependent slip-stick configurations. The formulation used to study these involves a singular integral equation in two variables which must be solved numerically, and because of the history dependence, requires in an incremental solution. Only crack lengths and coefficients of friction that result in a maximum of two slip or stick zones for any load location are considered in this paper. It is found that the maximum range of stress intensity factors occurs at the trailing crack tip.

Introduction

Steel wheel rims, rails, gear teeth, ball and roller bearings, cams, as well as other members involving a frictional interface and periodic contact loading are all subject to surface degradation. This may manifest itself in the form of pitting (crack originating at the surface), fretting, or spalling (crack originating below to surface). Spalling results from a crack growing parallel to the surface for some distance after which a transverse crack forms, ultimately leading to the detachment of a thin layer of material. These subsurface cracks may be initiated by preexisting defects such as inclusions, gas pores, or local soft spots, or may be generated during the cyclic straining process itself.

A subsurface crack under a static compressive load and a uniform normal pressure in various slip-stick configurations was studied by Chang, Comninou, Sheppard, and Barber [1]. An investigation of the stick-slip zones of a layer pressed on an elastic foundation subjected to a periodic tangential load was carried out by Comninou and Barber [2], but although history dependent, required no incremental formulation. Related static solutions are also given by Comninou et al. [3, 4].

Another contact problem, that of two semi-infinite elastic solids first pressed together, sheared and then at time $t=0$, subjected to a moving force pair at the interface, was studied by Dundurs and Gautesen [5]. A steady-state slip-stick configuration does not occur immediately upon application of the load and therefore a time-dependent solution had to be considered. However, the equations involved were invertible permitting a nonlinear integral equation in one variable to be developed for the unknown stick-slip boundary as a function of load position.

A preliminary study of a subsurface crack subjected to a moving load was carried out by Hearle and Johnson [6]. This problem is also history dependent, but the relevant equations cannot be inverted, hence a solution that involved small load steps, or increments was used. This particular study did not enforce the traction-free boundary condition on the surface of the half-plane and made other approximations which render the accuracy of the reported values of the Mode *II* Stress Intensity Factor (K_{II}) uncertain.

The present paper gives a more exact treatment of the subsurface crack lying parallel to the surface, subjected to a moving compressive normal surface force, as shown in Fig. 1. In particular, we explore the variation of maximum value of K_{II} and its range (ΔK_{II}) with the coefficient of friction (f) and the crack length/depth ratio (L/a). Because of the history dependence, the load sequence is not symmetric and one would not necessarily expect equal variation of K_{II} at the two crack tips.

The Problem Described

Consider the crack geometry depicted in Fig. 1 which represents a subsurface crack subjected to a moving compressive normal force. Distance t measures load position which varies monotonically, and is therefore a timelike variable. With the load P initially located far to the left of the origin, the crack will experience forward slip (top crack face

Contributed by the Applied Mechanics Division and presented at the Winter Annual Meeting, Miami, Fla., November 17–21, 1985 of THE AMERICAN SOCIETY OF MECHANICAL ENGINEERS.

Discussion on this paper should be addressed to the Editorial Department, ASME, United Engineering Center, 345 East 47th Street, New York, N.Y. 10017, and will be accepted until two months after final publication of the paper itself in the JOURNAL OF APPLIED MECHANICS. Manuscript received by ASME Applied Mechanics Division, July, 1984; final revision, April, 1985. Paper No. 85-WA/APM-15.

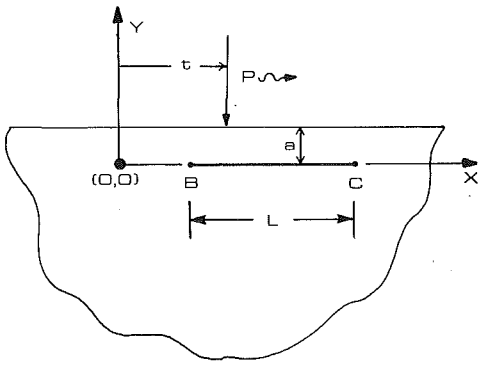

Fig. 1 Geometry of the problem

moving to the right relative to the unloaded crack) throughout its entire length, as shown in Fig. 2(*a*). As the load moves to the right (slowly enough for inertia effects to be ignored) the stress intensity factor K_{II} at both B (leading crack tip) and C (trailing crack tip) and the amount of forward shift continue to increase until the load is at position t_1. If the assumption of full forward slip were retained, further rightward load movement beyond t_1 would cause K_{II} at B to decrease, indicating backslip in a zone adjacent to B. This is inconsistent with the assumption and implies that a locked zone develops at crack tip B, as shown in Fig. 2(*b*).

As the load moves to the right of t_1 this locked zone will continue to grow until the entire crack length is locked (Fig. 2(*c*)), at which point the load is at location t_2. This locked configuration will be retained until load position t_3, where the shear traction at B exceeds the limiting value for backslip.

A backslip zone will grow to the right with additional load movement (Fig. 2(*d*)) until the entire crack is experiencing backslip (load position t_4 and Fig. 2(*e*)). During the initial growth of this backslip zone, there is a positive but decreasing forward shift. With further growth, shift will become increasingly negative until stick once again starts at B (load position t_5).

As the load is moved beyond position t_5, a scenario similar to that described in the foregoing ensues except that the direction of slip is reversed (compare Fig. 2(*a–d*) with Fig. 2(*e–h*)).

At load positions to the right of t_8 the entire crack is experiencing forward slip, as shown in Fig. 2(*i*). This condition results after the crack has been in a fully locked back-shifted configuration (Fig. 2(*g*)). As the load recedes to infinity, this backshift is relieved everywhere by forward slip, leaving the body free of residual stress.

If the crack is of sufficient length, forward slip can begin at B before the stick zone has reached C, giving rise to three or more zones. In this paper we restrict our investigation to cracks for which this does not occur. The two-zone cracks to be considered will be referred to as "short cracks." "Long cracks," which experience three or more zones at some load position(s), will be the subject of a subsequent paper.

Formulation

The problem is formulated by using the solution for a compressive load on an unflawed half-plane, corrected by an additional solution that ensures that appropriate boundary conditions are met along the crack [3, 4]. The unflawed half-plane shear and normal tractions are given by the Flamant solution.

The corrective term is represented by a distribution of edge dislocations of the glide type with density $B_x(x)$. This distribution depends on the position of the load, t, but the dependence is only indicated explicitly when needed for clarity.

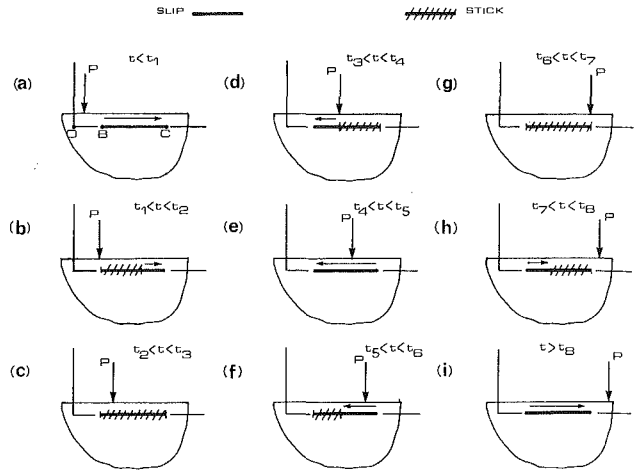

Fig. 2 Sequence of crack configurations as the load position changes

Combining the Flamant terms and the dislocation terms for both shear and normal tractions, we obtain:

$$S(x) = \frac{2Pa^2x_t}{\pi(a^2+x_t^2)^2} + \frac{2\mu}{\pi(\kappa+1)}\int_B^C B_x(\zeta)K_s(x,\zeta)d\zeta \tag{1}$$

$$N(x) = \frac{-2Pa^3}{\pi(a^2+x_t^2)^2} + \frac{2\mu}{\pi(\kappa+1)}\int_B^C B_x(\zeta)K_n(x,\zeta)d\zeta \tag{2}$$

where

$$K_s(x,\zeta) = \frac{1}{x-\zeta} + \frac{x-\zeta}{R}\left(-1+\frac{12a^2}{R}-\frac{64a^4}{R^2}\right) \tag{3}$$

$$K_n(x,\zeta) = \frac{8a^3}{R^2}\left(-3+\frac{16a^2}{R}\right) \tag{4}$$

$$R = 4a^2+(x-\zeta)^2$$

and $x_t = x-t$, μ is the shear modulus, and $\kappa = (3-4\nu)$ plane strain, with ν being Poisson's ratio.

The Mode *II* Stress Intensity Factors at B and C are

$$K_{II}(B) = -\lim_{x\to B}\left(\frac{2\mu}{\kappa+1}B_x(x)\sqrt{2\pi(x-B)}\right) \tag{5}$$

$$K_{II}(C) = \lim_{x\to C}\left(\frac{2\mu}{\kappa+1}B_x(x)\sqrt{2\pi(C-x)}\right) \tag{6}$$

The horizontal shift of the upper crack face relative to the lower face

$$h(x) = u(x,+0)-u(x,-0) \tag{7}$$

is related to $B_x(x)$ by

$$h(x) = -\int_B^x B_x(\zeta)d\zeta \tag{8}$$

We require continuity of displacements throughout the body except at the crack and hence

$$\int_B^C B_x(\zeta)d\zeta = 0 \tag{9}$$

The boundary conditions to be enforced along the crack depend on which of the configurations in Fig. 2 is being described and will be discussed in detail in the following sections, which have been labeled (2*a*)–(2*i*) to correspond with the figure. We assume that Coulomb friction occurs between the crack faces, governed by the equations and inequalities

$$S(x) = -fN(x);\quad \dot{h}>0;\quad \text{forward slip} \tag{10}$$

$$S(x) = fN(x);\quad \dot{h}<0;\quad \text{back slip} \tag{11}$$

$$\dot{h}=0;\quad |S(x)| \le -fN(x);\quad \text{stick}, \tag{12}$$

where $\dot{h}(x) = dh(x)/dt$ and $N(x) < 0$.

If the expressions for N and S from (1) and (2) are substituted into (10) and rearranged, we obtain

$$\frac{2\mu}{\pi(\kappa+1)}\int_B^C B_x(\zeta)[K_s(x,\zeta)+fK_n(x,\zeta)]d\zeta = \frac{2Pa^2(fa-x_t)}{\pi(a^2+x_t^2)^2} \tag{13}$$

(2*a*) Full Forward Slip ($t<t_1$). The full forward slip configuration is shown in Fig. 2(*a*) and is described by (10) enforced over the range $B<x<C$. Asymptotic analysis by Dundurs and Comninou [7] shows that $B_x(x)$ is square root singular at both tips under full forward slip. Putting equations (9) and (13) into dimensionless form by the change of variables:

$$\delta = (C-B)/(2a); \qquad \sigma = (B+C)/(2a) \tag{14}$$

where

$$\zeta/a = \delta r + \sigma; \qquad x/a = \delta s + \sigma \tag{15}$$

and letting

$$B_x(r) = \frac{P(\kappa+1)}{2\mu a}(1-r^2)^{-1/2}\phi(r) \tag{16}$$

and by discretizing the resulting singular integral equations according to the numerical method of Erdogan, Gupta, and Cook [8], the following series of equations is obtained:

$$\sum_{i=1}^{n}\frac{\phi(r_i)}{n}\left[\frac{1}{(s_k-r_i)}+K(s_k,r_i)\right] = \frac{2[f-(\delta s_k+\sigma)]}{\pi[1+(\delta s_k+\sigma)^2]^2} \tag{17}$$

$$k=1,\ldots,n-1$$

$$\sum_{i=1}^{n}\frac{\phi(r_i)}{n}=0 \tag{18}$$

where

$$r_i=\cos\left(\frac{2i-1}{2n}\pi\right); \quad i=1,\ldots,n$$

$$s_k=\cos\left(\frac{k}{n}\pi\right); \quad k=1,\ldots,n-1 \tag{19}$$

The n equations represented by (17) and (18) are sufficient for finding the n unknowns $\phi(r_i)$.

The stress intensity factors are obtained by substituting (16) into (5) and (6) as

$$\left(\frac{\pi a^{1/2}}{2P}\right)K_{II}(B) = -\sqrt{2}(\pi/2)^{3/2}\delta^{1/2}\phi(-1) \tag{20}$$

$$\left(\frac{\pi a^{1/2}}{2P}\right)K_{II}(C) = \sqrt{2}(\pi/2)^{3/2}\delta^{1/2}\phi(+1) \tag{21}$$

Values of $\phi(\pm 1)$ are found using the interpolation technique proposed by Krenk [9]. The stress intensity factor at B, given by (20) increases with t until a maximum is reached at $t=t_1$, after which a stick zone starts to develop at B.

(2*b*) Growing Stick Zone ($t_1<t<t_2$). After $K_{II}(B)$ has peaked, a stick zone grows from B toward C upon further load movement. As the transition from stick to slip moves, for example from m_1 to m_2, the dislocation distribution in $m_1<x<m_2$ will be locked in. These locked in dislocations, along with those in the range $B<x<m_1$, will continue to affect shear and normal tractions developed in $m_2<x<C$ even though they have become inactive. It is this continued influence of locked in dislocations that makes the problem history dependent. The approach taken in the following is similar to that developed by Dundurs and Gautesen [5].

For a growing stick zone and a forward slip zone with transition at point m, condition (10) is observed in the range $m<x<C$, while condition (12) prevails in $B<x<m$. Equation (13) is to be integrated over *all* dislocations $B<x<C$, not just those in the slip zone. However, as previously stated, the dislocations in the zone $B<x<m$ are locked in place, and therefore are unaffected by load movement to the right, i.e., $\dot{B}_x = dB_x(\zeta,t)/dt = 0$; $B<\zeta<m$. Differentiating (9) and (13) with respect to t therefore allows the lower bound of integration to be changed from B to m. The resulting equations are

$$\frac{2\mu}{\pi(\kappa+1)}\int_m^C \dot{B}_x(\zeta,t)[K_s(x,\zeta)+fK_n(x,\zeta)]d\zeta = \frac{2Pa^2[4fax_t-3x_t^2+a^2]}{\pi(a^2+x_t^2)^3} \qquad m<x<C \tag{22}$$

$$\int_m^C \dot{B}_x(\zeta,t)d\zeta = 0 \tag{23}$$

Asymptotic analysis [7, 10] shows that the shear tractions must have continuous derivatives with respect to t at m, the transition point between a growing stick zone and a slip zone. Therefore, $\dot{B}_x$ in (22) and (23) is singular at C, and bounded at m and can be represented using a dimensionless formulation for the range $m<x<C$ as:

$$\dot{B}_x(r,t) = \frac{P(\kappa+1)\gamma(r,t)(1+r)^{1/2}}{2\mu a^2(1-r)^{1/2}} \tag{24}$$

where r is given by (15) with δ and σ redefined as

$$\delta = (C-m)/(2a); \qquad \sigma = (C+m)/(2a) \tag{25}$$

Substituting (24) into (22) and (23), and discretizing we find

$$\sum_{i=1}^{n}\frac{2(1+r_i)}{2n+1}\gamma(r_i)[K_s(r_i,s_k)+fK_n(r_i,s_k)] = \frac{2\{4f(\delta s_k+\sigma-t)-3(\delta s_k+\sigma-t)^2+1\}}{\pi(1+(\delta s_k+\sigma-t)^2)^2}; \quad k=1,\ldots,n \tag{26}$$

$$\sum_{i=1}^{n}\frac{2(1+r_i)}{2n+1}\gamma(r_i)=0 \tag{27}$$

where

$$r_i=\cos\left(\frac{2i-1}{2n+1}\pi\right); \quad i=1,\ldots,n$$

$$s_k=\cos\left(\frac{2k}{2n+1}\pi\right); \quad k=1,\ldots,n \tag{28}$$

Relationships (26) and (27) represent $(n+1)$ equations for the n values of $\gamma(r_i)$ and the transition point m, if the load position t is assumed known. The relation between m and t has to be found by iteration using equation (27) and it is numerically more efficient to fix m and iterate on t rather than vice versa. In this way, the points r_i and s_k, and the kernel matrix have to be calculated only once per step, since only the right-hand side of (26) is affected by the value of t.

The second reason for preferring this approach concerns the history dependence of the problem. Because (26) and (27) have no closed-form solution, the problem must be solved numerically as a series of small load and transition point increments. During this incremental process the effect of the currently active dislocations on shear and normal tractions is continually added to a running total of the effect of *all* dislocations (both locked and active) on shear and normal tractions at a series of fixed "tracer" points. By choosing these "tracer" points as the known m values, the numerical

evaluation of the traction increments is simplified (see the following).

A check is made at each step to ensure that shift in the currently active zone is in the forward direction. Equation (8) can be written in terms of $\dot{B}_x$, using (9) as:

$$\dot{h}(x) = \int_x^C \dot{B}_x(\zeta)\, d\zeta \tag{29}$$

the right-hand side of which can be evaluated using the trapezoidal rule.

Now that the load position t is known corresponding to the transition point m and the current distribution, the increment in shear and normal tractions at any x caused by the most recent movement in load and transition point can be found. In developing this incremental solution, it is helpful to refer to the current transition and load position as m_{j+1} and t_{j+1}, respectively, and to the previous points as m_j and t_j. The increment ΔS_d in shear traction caused by the load movement from t_j to t_{j+1} can be written as

$$\Delta S_d(x,t) = \frac{2\mu}{\pi(\kappa+1)} \int_{t_j}^{t_{j+1}} \int_{m(z)}^{C} \dot{B}_x(\zeta,z) K_s(x,\zeta)\, d\zeta\, dz \tag{30}$$

where $\dot{B}_x(\zeta, z)$ refers to the derivative of the dislocations that are active when the transition point is at $m(z)$. Remembering that

$$\dot{B}_x(\zeta,z) = \frac{P(\kappa+1)\gamma(\zeta,z)(\zeta - m(z))^{1/2}}{2\mu a^2 (C-\zeta)^{1/2}} \tag{31}$$

the order of integration can be interchanged in (30). The integration with respect to z, the load position dummy variable, can be performed if $\gamma(\zeta,z)$ is assumed to remain constant for a small change in z, and the relationship between m and z is approximated by the piecewise linear form

$$m(z) = m_j + (z - t_j)\frac{(m_{j+1} - m_j)}{(t_{j+1} - t_j)}; \quad m_j < m(z) < m_{j+1} \tag{32}$$

This procedure is used because the term $(\zeta - m(z))^{1/2}$ in $\dot{B}_x$ would give discontinuities in slope at the points m_j if the simpler, piecewise constant integration were used.

We also note that the dislocations in the range $m_j < \zeta < m_{j+1}$ only remain active while $t_j < s < t^*$, where t^* $(< t_{j+1})$ refers to the load position when $m(s) = m_{j+1}$ and can be found from equation (32). Using these results and performing the integration with respect to z gives

$$\Delta S_d(x,t) = \frac{-2(t_{j+1} - t_j)}{3\pi(m_{j+1} - m_j)} \int_{m_j}^{C} \frac{\gamma(\zeta) K_s(\zeta,x)}{(C-\zeta)^{1/2}} [(\zeta - m^*)^{3/2} - (\zeta - m_j)^{3/2}]\, d\zeta \tag{33}$$

where

$$m^* = \zeta; \quad m_j < \zeta < m_{j+1}$$
$$= m_{j+1}; \quad m_{j+1} < \zeta < C. \tag{34}$$

In dimensionless, discretized form, (33) becomes

$$\Delta S_d(x,t)\left(\frac{a}{P}\right) = \frac{-2(t_{j+1} - t_j)}{3(m_{j+1} - m_j)} \sum_{i=1}^{n} \frac{2(1+r_i)}{2n+1} \gamma(r_i) K_s(r_i, s_k) \delta \left[\frac{(r_i - r^*)^{3/2}}{(r_i+1)^{1/2}} - (r_i+1)\right] \tag{35}$$

where

$$r^* = r_i; \quad m_j < a(\delta r_i + \sigma) < m_{j+1}$$
$$= (m_{j+1}/a - \sigma)/\delta; \quad m_{j+1} < a(\delta r_i + \sigma) < C. \tag{36}$$

An expression for the increment in normal tractions N_d can be developed in an analogous manner.

The increment in the shear tractions can be evaluated directly at any point outside of the interval $m_j < x < C$, but *within* this interval, equation (33) is a Cauchy singular integral and the numerical integration procedure is accurate only at the specified collocation points. However, the kernel of the corresponding integral for the increment in normal tractions is bounded for all x and hence condition (10) can be used to evaluate the shear increment at points in the interval $m_{j+1} < x < C$. The technique proposed by Sheppard and Comninou [11] was used to find the shear tractions at a tracer point near B during the first increment only. It was not needed for subsequent increments because the tracer points were chosen to coincide with the transition points.

The change in K_{II} at C caused by an incremental change in the transition point is:

$$\left(\frac{\pi a^{1/2}}{2P}\right) \Delta K_{II}(C) = \pi^{3/2} \delta^{1/2} \gamma(+1)(t_{j+1} - t_j) \tag{37}$$

As the transition point, m, between stick and forward slip is incremented from $B < x < C$ the relationship between S and N in the interval $B < x < m$ is continually monitored to ensure that condition (12) is satisfied. If a violation is found just to the right of B before m has reached C, we are no longer dealing with a "Short Crack" and there will be three zones along the crack: namely backslip in $B < x < q$ such that $B < q < m$, stick in $q < x < m$, and forward slip in $m < x < C$.

The load location t at which the crack has just reached the configuration of full stick is denoted by t_2. Convergence of the incremental procedure was checked by finding $K_{II}(C)$ at $t = t_2$ as a function of the number of incremental steps (e.g., 25 increments were required for convergence for $L/a = 1.00$).

(2C) Full Stick ($t_2 < t < t_3$). Once the load has passed the point t_2, full stick occurs and the solution is obtained by simply updating the contribution from the Flamant solution, while keeping the contribution from the locked in dislocations unchanged. This condition persists until inequality (12) is violated. The nature of this violation is always such as to indicate the development of a backslip zone at B. The load position at which this occurs is denoted by t_3.

(2d) Growing Backslip Zone ($t_3 < t < t_4$). An incremental solution is not required for the growing backslip zone depicted in Fig. 2(*d*). The shear and normal tractions can be written in the form

$$S(x) = \frac{2\mu}{\pi(\kappa+1)} \int_B^q \Delta B_x(\zeta) K_s(x,\zeta)\, d\zeta + \frac{2Pa^2 x_t}{\pi(a^2 + x_t^2)^2} + S_d(x) \tag{38}$$

$$N(x) = \frac{2\mu}{\pi(\kappa+1)} \int_B^q \Delta B_x(\zeta) K_n(x,\zeta)\, d\zeta - \frac{2Pa^3}{\pi(a^2 + x_t^2)^2} + N_d(x) \tag{39}$$

where $S_d(x)$, $N_d(x)$ are the contributions from the dislocations locked in during the preceding full-stick phase, and ΔB_x are the additional dislocations describing the backslip and hence located in the backslip zone defined as $B < x < q$.

Equation (11) is valid in $B < x < q$, and hence, substituting from (38) and (39)

$$\frac{2\mu}{\pi(\kappa+1)} \int_B^q \Delta B_x(\zeta)[K_s(x,\zeta) - f K_n(x,\zeta)]\, d\zeta = f N_d(x) - S_d(x) - \frac{2Pa^2(fa + x_t)}{\pi(a^2 + x_t^2)^2}; \quad B < x < q \tag{40}$$

Also, to comply with equation (9), we require

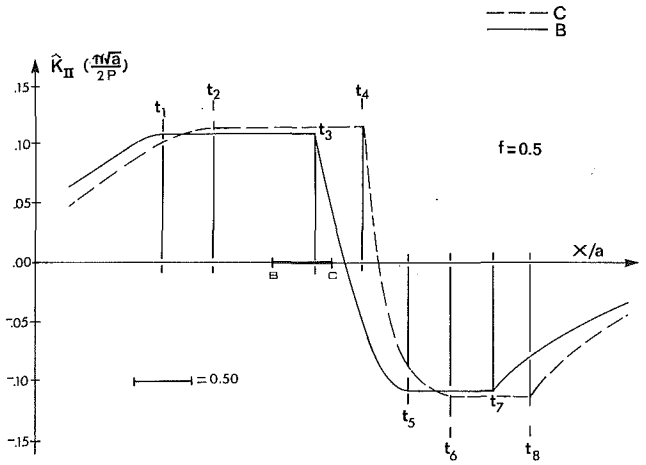

Fig. 3 Stress intensity factors as a function of load position for $L/a = 0.5$; $f = 0.5$. The solid line BC represents the extent of the crack.

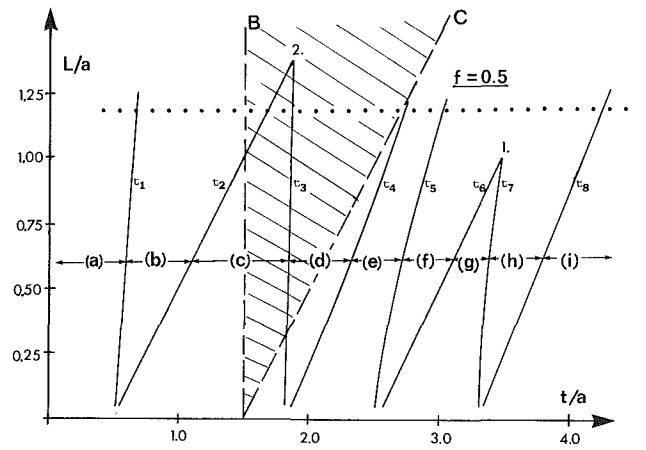

Fig. 4 The transitional load positions t_1, t_2, etc. as functions of crack length L/a for $f = 0.5$. The crack extends between the dashed lines B and C.

$$\int_B^q \Delta B_x(\zeta)\, d\zeta = 0 \tag{41}$$

This currently active distribution of dislocations is singular at the crack tip B and bounded at the stick-slip transition q. We therefore use the representation

$$\Delta B_x(r) = \frac{P(\kappa+1)(1-r)^{1/2}}{2\mu a(1+r)^{1/2}}\,\phi(r) \tag{42}$$

Equations (40) and (41) can then be normalized and discretized, giving $(n+1)$ equations for finding the n values of $\phi(r_i)$ and the load position t for a specified value of q, $B<q<C$. Note that the tractions S_d, N_d are known only at the tracer points m_j. However, they are smooth functions of x and a cubic spline fit is sufficient to give the values at the points s_k.

The change in K_{II} at B from its locked value can also be found:

$$\left(\frac{\pi a^{1/2}}{2P}\right)\Delta K_{II}(B) = -(\pi)^{3/2}\delta^{1/2}\phi(-1) \tag{43}$$

The backslip zone will continue to grow until $q = C$, for which the corresponding load position is denoted by t_4.

(2e) Full Backslip ($t_4 < t < t_5$). When the transition point between growing backslip and stick has reached C, the crack experiences full backslip (Fig. 2(*e*)). Once this condition occurs, the problem ceases to be history dependent, since there are no remaining locked-in dislocations. The for-

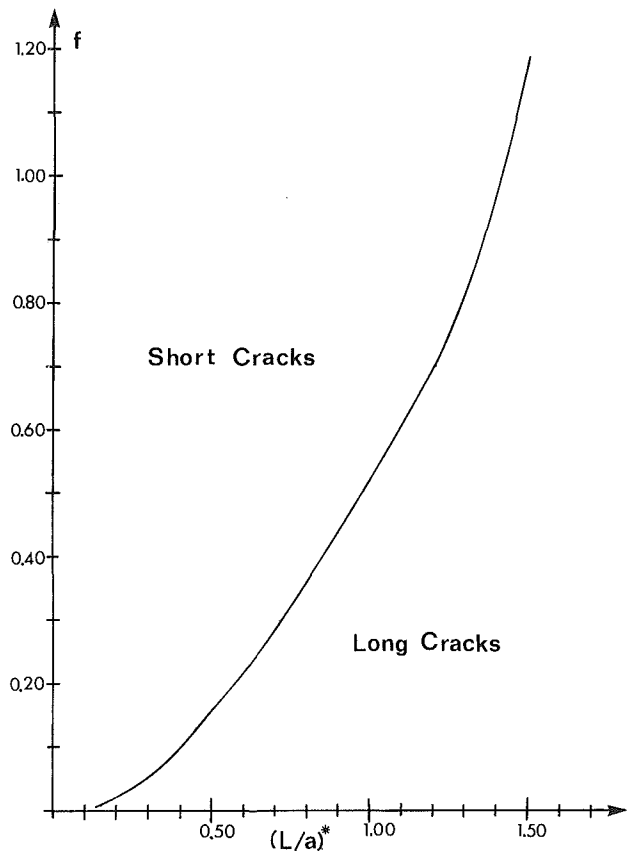

Fig. 5 The critical crack length as a function of crack face coefficient of friction f. Short cracks are those that never experience more than two zones.

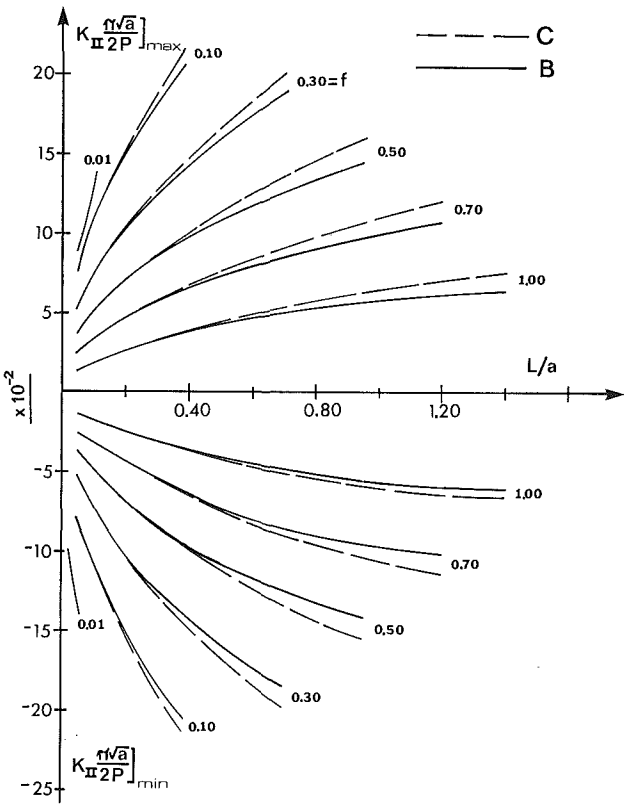

Fig. 6 Maximum and minimum values of stress intensity factors at B and C as functions of crack length L/a for various coefficients of friction

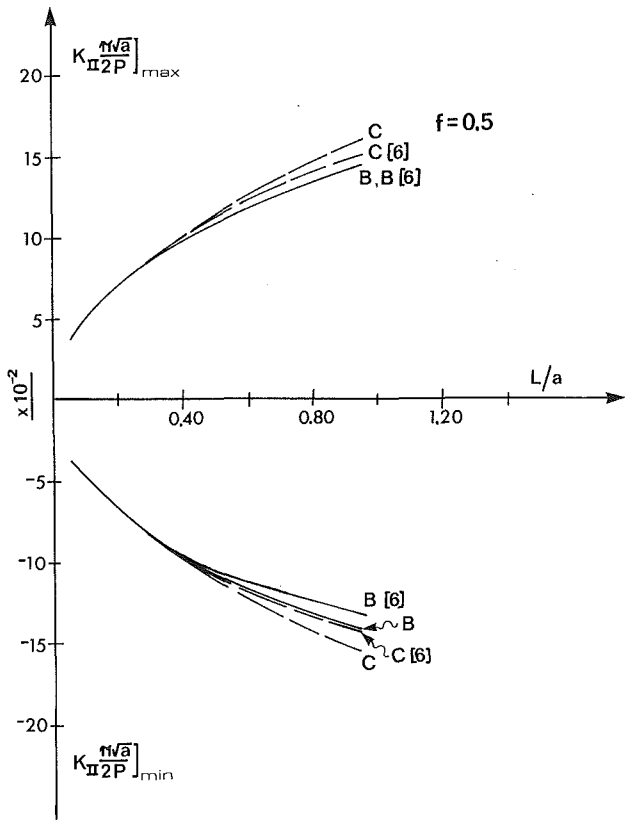

Fig. 7 Comparison of maximum stress intensity factors with the approximate solution of Hearle and Johnson [4]; $f = 0.5$

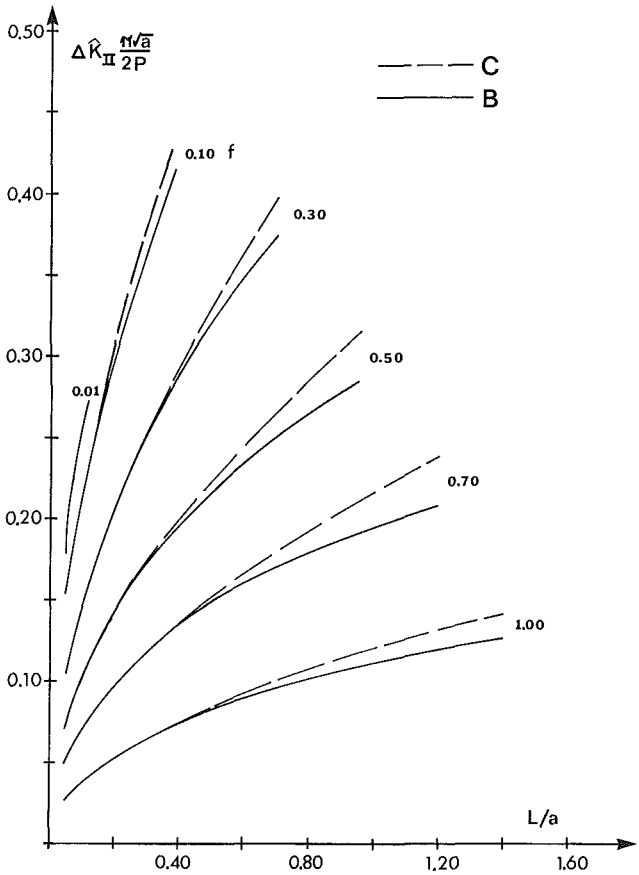

Fig. 8 Effect of crack length L/a on the range of stress intensity factors K_{II} for various coefficients of friction

mulation is identical to that for full forward slip (Section (2*a*)) except that condition (10) is replaced by (11), which is formally equivalent to changing the sign of f in the appropriate equations.

Full backslip persists as long as the solution satisfies

$$\dot{h}(x) < 0; \qquad B < x < C. \tag{44}$$

As in Section (2*a*), this is first violated at B and corresponds to $K_{II}(B)$ reaching a maximum negative value at load position $t = t_5$.

It is interesting to note that (44) is a necessary but not sufficient condition for full backslip to occur, if the previous history is not considered. The load position t_4 at which full backslip starts is determined by the previous history of the process, but the memory of the system is then erased.

(2*f*–*i*) Subsequent Phases ($t > t_5$). After the load passes the point t_5, the crack passes through a sequence of conditions shown in Figs. 2(*f*)-(*i*), which are essentially identical to 2(*b*–*e*), except that the direction of slip is reversed. The formulations used are identical except for a change of sign of f in appropriate equations.

The final phase ($t > t_8$) is one of full forward slip (Fig. 2(*i*)) as the load recedes to infinity, leaving the body in a stress-free state.

Results

The formulation described in the foregoing can be used to explore the variation of stress intensity factors, K_{II}, at B and C with load position t. Figure 3 shows the results obtained for $L/a = 0.5$ and $f = 0.5$. The horizontal portions of the curves correspond to periods when there is a stick zone adjacent to the appropriate crack tip. Each tip experiences a positive and a negative locked period, which represent the maximum and minimum value respectively of K_{II}. The transition points t_1, t_2, etc., mark the beginnings and ends of these periods. Notice that the curves have continuous slope at transitions from slip to stick, but discontinuous slope at transitions from stick to slip.

Similar results were obtained for a range of crack lengths (L/a) and the effect of this parameter on the load locations for the various transitions is illustrated in Fig. 4 for $f = 0.5$. The dashed lines represent the locations of the crack tips B and C.

The lines defining the transitions t_6, t_7 intersect at the point labeled 1 in Fig. 4, corresponding to $L/a = 0.96$. This is the maximum length of crack that can be considered short for $f = 0.5$. Cracks longer then this critical value will start to slip forward at B in configuration 2*f* before the backslip zone at C has shrunk to zero.

A similar intersection between t_2, t_3 occurs at point 2, where $L/a > 1.4$. Cracks in the range $0.96 < L/a < 1.4$, such as that described by the dotted line in Fig. 4 will follow the sequence described in the paper for the first half of the cycle until a three region configuration is developed some time after t_5.

The critical value of crack length $(L/a)^*$, corresponding to point 1 in Fig. 4, was found for coefficients of friction in the range $0.01 < f < 1.1$ and the results are presented in Fig. 5.

The maximum and minimum values of K_{II} at B and C are shown in Fig. 6 as a function of crack length for various coefficients of friction. In each case, the curves are terminated at the critical crack length $(L/a)^*$ defined in Fig. 5. In all cases, increasing crack face friction has a very marked effect in decreasing stress intensity factors, as we would expect. For very short cracks the curves for tips B and C coincide and are symmetrical about zero, indicating that all four extreme values have approximately equal magnitude. These magnitudes increase with crack length, but the values at C become significantly greater than those at B and some asymmetry is developed.

The results for $f=0.5$ are compared with the approximate solution of Hearle and Johnson [6] in Fig. 7. Their approximation consists of:

(*i*) Using the dislocation solution for the full plane and hence neglecting the influence of the free surface;
(*ii*) Using an inexact model of the locked regions of the crack.

Figure 7 shows that their results are accurate for very short cracks but become less accurate as crack length increases, as we should expect. For longer cracks, their estimates of $K_{II}(B)$ are still very good (within 3 percent) but those of $K_{II}(C)$ are less good (up to 8 percent underestimated). This can be explained by referring to those stages of the solution procedure at which extreme values of K_{II} are obtained. In each case, the maximum of $K_{II}(B)$ follows a period of full slip; the maximum occurs at t_1 following full forward slip and the minimum at t_5 following full backslip. It follows that the estimates of these quantities in [6] are affected only by their approximation (*i*), since no stick zones are involved. By contrast, when $K_{II}(C)$ reaches a maximum (t_2, t_6) there is stick throughout the crack and we conclude that approximation (*ii*) is responsible for the less good estimates of this quantity.

Of particular importance for crack growth is the range of K_{II} (i.e., $\Delta K_{II}=(K_{II\max}-K_{II\min})$), which is shown in Fig. 8. Except for very short cracks, this range is significantly greater at C than at B, indicating a tendency for cracks to grow from the trailing edge under repeated loading; a conclusion that is supported by the experimental evidence of Yoshimura, Rubin, and Hahn [12].

Conclusions

The method described enables the stress field to be found near a subsurface crack subjected to a load moving over the surface. Coulomb friction between the crack faces has a substantial effect in reducing the stress intensity factors at the crack tips and introduces history dependence into the problem.

The stress intensity factors are found to reach higher maximum values at the trailing tip than at the leading tip; a result that is supported by experimental evidence showing that such cracks tend to propagate preferentially from the trailing tip.

The predictions of a previous approximate solution by Hearle and Johnson [6] are shown to be very good for the leading tip, but to underestimate the stress intensity factor at the trailing tip, except for very short cracks.

Acknowledgment

Support by the Office of Naval Research through the contract N00014-K-0287 during the course of this research is gratefully acknowledged.

References

1 Chang, F.-K., Comninou, M., Sheppard, S., and Barber, J. R., "The Subsurface Crack under Conditions of Slip and Stick Caused by a Surface Normal Force," ASME JOURNAL OF APPLIED MECHANICS, Vol. 51, 1984, pp. 311-316.

2 Comninou, M., and Barber, J. R., "Frictional Slip Between a Layer and a Substrate Due to a Periodic Tangential Surface Force," *Int. J. of Solids Structures*, Vol. 19, 1983, pp. 533-539.

3 Comninou, M., Schmueser, D., and Dundurs, J., "Frictional Slip Between a Layer and a Substrate Caused by a Normal Load," *Int. J. Eng. Sci.*, Vol. 18, 1980, pp. 131-137.

4 Comninou, M., Schmueser, D., and Dundurs, J., "Separation and Slip Between a Substrate Caused by a Tensile Load," *Int. J. Eng. Sci.*, Vol. 18, 1980, pp. 1149-1155.

5 Dundurs, J., and Gautesen, A. K., "On the Approach to Steady State for Frictional Contact Under Moving Loads," ASME JOURNAL OF APPLIED MECHANICS, Vol. 50, 1983, pp. 783-788.

6 Hearle, A. D., and Johnson, K. L., "Mode *II* Stress Intensity Factors for a Crack Parallel to the Surface of an Elastic Half-Space Subjected to a Moving Point-Load," submitted to *Journal Mech. Phys. Solids*.

7 Dundurs, J., and Comninou, M., "Some Consequences of the Inequality Conditions in Contact and Crack Problems," *J. Elasticity*, Vol. 9, 1979, pp. 71-82.

8 Erdogan, F., Gupta, G. D., and Cook, T. S., in: *Methods of Analysis and Solution of Crack Problems*, Noordhoff, Leyden, 1973.

9 Krenk, S., "On the Use of the Interpolation Polynomial for Solutions of Singular Integral Equations," *Q. Appl. Math.*, Vol. 32, 1975, pp. 479-484.

10 Comninou, M., Barber, J. R., and Dundurs, J., "Interface Slip Caused by a Surface Load Moving at a Constant Speed," *Int. J. Mech. Sci.*, Vol. 25, 1983, pp. 41-46.

11 Sheppard, S. D., and Comninou, M., "On the Interpolation of Cauchy Integrals," in *Numerical Solution of Singular Integral Equations*, Gerasoulis, A., and Vichnevetsky, R., eds., IMACS, 1984.

12 Yoshimura, H., Rubin, C. A., and Hahn, G. T., "Cyclic Crack Growth Under Repeated Rolling Contact," prepared for Eleventh Canadian Fracture Conference, University of Ottawa, Ontario, Canada, 1984.